

NOTE: This is a draft of a paper being submitted for publication. Contents of this paper should not be quoted nor referred to without permission of the author(s).

NEUTRON DAMAGE CALCULATIONS IN Cu, Nb AND Au TO 32 MeV:
APPLICATION TO SPUTTERING AND DEUTERON-BREAKUP NEUTRON SOURCES

J. B. Robertc, M. T. Robinson and C. Y. Fu

MASTER

By acceptance of this article, the publisher or recipient acknowledges the U. S. Government's right to retain a non-exclusive, royalty-free license in and to any copyright covering the article.

SOLID STATE DIVISION
OAK RIDGE NATIONAL LABORATORY
Operated by
UNION CARBIDE CORPORATION
for the
ENERGY RESEARCH AND DEVELOPMENT ADMINISTRATION
Oak Ridge, Tennessee

February 1976

NOTICE
This report was prepared as an account of work sponsored by the United States Government. Neither the United States nor the United States Energy Research and Development Administration, nor any of their employees, nor any of their contractors, subcontractors, or their employees, make any warranty, express or implied, or assume any legal liability or responsibility for the accuracy, completeness or usefulness of any information, apparatus, product or process disclosed, or represents that its use would not infringe privately owned rights.

DISTRIBUTION OF THIS DOCUMENT IS UNLIMITED

fy

NEUTRON DAMAGE CALCULATIONS IN Cu, Nb AND Au TO 32 MeV: *
APPLICATION TO SPUTTERING AND DEUTERON-BREAKUP NEUTRON SOURCES

J. B. Roberto, M. T. Robinson and C. Y. Fu
Oak Ridge National Laboratory
Oak Ridge, Tennessee 37830

ABSTRACT

Primary recoil distributions and specific damage energies have been computed for high energy deuterium-breakup neutrons in Cu, Nb and Au. The calculations are based on theoretical neutron cross sections, and consider in particular a d-Be spectrum broadly peaked at 15 MeV with some neutrons above 30 MeV. The theoretical results are similar to corresponding calculations for monoenergetic 15-MeV neutrons, and are in good agreement with range measurements of $(n,2n)$ recoils generated by high energy d-Be neutrons in Nb and Au. The calculations are also consistent with recent d-Be neutron sputtering experiments in Nb and Au and demonstrate the usefulness of deuterium-breakup neutron sources for simulating fusion neutron effects.

* Research sponsored by the U. S. Energy Research and Development Administration under contract with Union Carbide Corporation.

1. Introduction

The use of high energy neutrons from the deuteron-breakup reaction presents an attractive possibility for simulating the 15-MeV component of a fusion reactor neutron spectrum. A deuteron-breakup source offers advantages in flux and experimental volume over other proposed sources, but is characterized by a neutron spectrum which is broadly distributed in energy compared with the monoenergetic distribution characteristic of d-T fusion. In this paper, we explore the effects of this broad energy distribution on the corresponding primary recoil spectra and damage energies for a typical deuteron-breakup neutron source. The theoretical results are correlated with experimental data from recent measurements [1] of sputtering yields and ranges of (n,2n) recoils resulting from high energy d-Be neutrons in Nb and Au. Particular attention is given to the discussion of high energy neutron sputtering using deuteron-breakup sources.

Neutron energy distributions for the deuteron-breakup reaction in Li and Be are shown in Fig. 1. These distributions are for a deuteron energy of 40 MeV, and are based on recent time-of-flight measurements [2] for neutrons emitted in the forward direction. Both the d-Li and d-Be spectra are broadly peaked near 15 MeV with some neutrons above 30 MeV. The present calculations were undertaken in order to interpret sputtering and radiation effects from such neutron sources. Earlier treatments [3,4] of high energy neutron damage have been based on cross sections from nuclear data files such as ENDF/B [5] and therefore limited to neutron energies below 20 MeV. We have used theoretical nuclear data [6] to extend calculations of recoil spectra and damage energy in Cu, Nb, and Au to 32 MeV.

2. Damage Calculations

2.1 Theory and Energy Dependence. The details of the nuclear physics [6] and damage calculations [7] have been treated elsewhere, and will be described only briefly here. The possible nuclear reactions are divided into four groups: elastic scattering and nonelastic interactions where a neutron, a proton, or an alpha particle is the first particle emitted. Subsequent particle emissions in nonelastic events are ignored. Above a few MeV, the elastically-scattered neutrons are strongly peaked in the forward direction, reducing the relative elastic contribution to the average recoil energy. The nonelastic recoils are peaked at one-fourth the maximum possible recoil energy, which corresponds to the maximum kinematically allowed inelasticity. This peaking of nonelastic recoils at $T_{\max}/4$ also corresponds to low emitted particle energies, which supports our assumption that subsequent particle emissions can be neglected. Primary recoil probability densities for (n,n') and (n,nx) events in Au are shown in Fig. 2 for several neutron energies.

Damage energies [3] were derived from the recoil calculations using the Lindhard [8] theory of electronic stopping. The damage energy is that part of the primary recoil energy which is ultimately available for producing atomic displacements, and is useful in the description of both sputtering and bulk effects. The calculated damage energies for the various nuclear reactions were multiplied by the corresponding interaction cross sections to obtain a specific damage energy per neutron. The resulting total specific damage energies for Cu, Nb and Au are shown in Fig. 3 for neutron energies up to 32 MeV. The relative elastic and

inelastic $[(n,n') + (n,nx)]$ contributions in Au are also shown in the figure. At 15 MeV, the damage energies from these calculations agree well with values [3,4] derived from ENDF/B data.

2.2 Results for d-Be Neutrons. The results of the above calculations were used to generate primary recoil spectra and specific damage energies for high energy d-Be neutrons in Cu, Nb and Au. The particular d-Be spectrum considered is shown in Fig. 1, and the calculated recoil distributions for this spectrum are compared with the corresponding distributions for monoenergetic 15-MeV neutrons in Figs. 4 and 5. In Fig. 4, the primary recoil spectrum for Nb is also compared with a calculated [9] recoil distribution for the first wall of a typical d-T fusion reactor.

The recoil energy distributions of Figs. 4 and 5 are quite similar for the d-Be and 15-MeV source, each dominated by elastic scattering at low recoil energies with a broad shoulder due to nonelastic interactions at higher energies. Specific damage energies derived from the recoil distributions are also nearly the same for d-Be and 15-MeV neutrons, as shown in Table 1. On the other hand, both the d-Be and 15-MeV recoil spectra for Nb are considerably harder than the corresponding distribution for a fusion reactor first wall, a consequence of the large fraction of lower energy reflected neutrons in the reactor spectrum (see Fig. 1).

It is interesting to note that the d-Be neutrons produce recoil spectra which are actually softer than the 15-MeV spectra over much of the range of higher energy recoils. This is apparent in Figs. 4 and 5, even though approximately one-half of the d-Be neutrons are more energetic than 15 MeV. These higher energy neutrons, however, tend to produce relatively fewer high energy recoils since the nonelastic scatterings are

spread over a wider range of possible recoil energies. This effect can be seen by replotting the recoil probability densities of Fig. 2 using an absolute energy abscissa. The relative peak heights for the higher energy neutrons will be reduced in proportion to their increase in absolute energy width, accounting for the reduced fraction of higher energy recoils.

3. Comparisons with Experiment

3.1 Ranges of $(n,2n)$ Recoils. A good indication of the reliability of the recoil calculations may be obtained by comparing experimental ranges of primary recoils generated by d-Be neutrons with theoretical ranges based on the calculated recoil energies. We have made this comparison for radioactive recoils resulting from $(n,2n)$ reactions in d-Be irradiated Nb and Au. The experimental results were obtained during a recent neutron sputtering measurement [1] using procedures which have been described elsewhere [10]. The idea of the experiment is shown in Fig. 6. The number of radioactive recoils collected on graphite catcher foils is compared with the remaining activity in the target. The emitted fraction of $(n,2n)$ activity from the forward surface of the target foil is a direct measure of the projected range of the recoils.

The formalism for interpreting range measurements using radioactive recoils has been given recently by Gähler, Kalus, and Behrisch [11]. An important consideration in the measurements is the angular distribution of the starting recoils. In our d-Be irradiations, the neutrons are emitted in a forward-directed cone with an average semi-apex of 11° . Subsequent spreading of the recoils from the two neutron emissions is about 20° , assuming independent isotropic center-of-mass emissions. For the recoil energies considered here, the projected ranges are insensitive to

uncertainties of this order in the starting angle, and the error in range introduced by the spreading is less than 10%. Theoretical ranges for the recoils were derived from the tabulation of range distributions by Winterbon [12]. These calculations are appropriate for an infinite solid, but for the considered recoil energies the effect of introducing a real surface can probably be neglected.

The experimentally-determined ranges are compared with theoretical calculations for self-ions in Nb and Au in Table 2. For the purposes of this comparison, the average recoil energies were determined by weighting the calculated recoil distributions over the (n,2n) activation spectrum using ENDF/B [5] cross sections. It was assumed that the (n,2n) recoil energy distributions were given by our [(n,n') + (n,nx)] results. The (n,2n) reaction accounts for the majority of the high energy recoils in Nb and Au, and the close agreement between theory and experiment suggests that our theoretical calculations of recoil energies are reasonable. These measurements are consistent with corresponding results [11] obtained using 14-MeV neutrons.

3.2 Sputtering Yields. The theoretical sputtering yield is proportional to the deposited energy and can be written [13,14]

$$S = \frac{0.042}{(\text{\AA}^2)} \frac{\langle \sigma \hat{E} \rangle}{U_0} \quad (1)$$

where S is the forward sputtering yield for a beam geometry, $\langle \sigma \hat{E} \rangle$ is the specific damage energy, and U_0 is the surface binding energy (usually taken as equal to the heat of sublimation). Calculated sputtering yields based on our theoretical damage energies are compared with the results

of a recent d-Be neutron sputtering experiment [1] in Table 1. The theory is consistent with the experimental results in both Nb and Au. The damage energy calculations are also in good agreement with recent bulk damage experiments in Cu and Nb [15] using high energy d-Be neutrons.

4. Discussion

The good agreement between theory and experiment obtained for the recoil ranges and sputtering yields described above indicates that we can interpret high energy neutron interactions using our theoretical approach. The results are also useful in establishing the relevance of d-Be neutron sputtering experiments to the simulation of 15-MeV neutron sputtering. The sputtering process is initiated by the primary recoil spectrum, and as we have seen in Figs. 4 and 5, differences between recoil spectra for d-Be and 15-MeV neutrons are small. Furthermore, the calculations indicate that spike effects [13] from energetic recoils which would increase yields should be comparable for the two sources. Actually, the good agreement between the calculated and measured forward yields in Au suggests that these effects may not be important at fusion neutron energies. On the other hand, the backward sputtering yields reported for Au [1] are much higher than expected from theory [14], however, much of this discrepancy can be attributed to the initial spread in primary recoil directions.

The damage calculations described above are also relevant to the broader question of the simulation of fusion neutron effects using deuteron-breakup neutron sources. The results indicate that spectral differences between monoenergetic 15-MeV neutrons and deuteron-breakup neutrons peaked at the same energy are not strongly reflected in the

Corresponding primary recoil distributions and damage energies. Overall, the calculations suggest that neutron damage effects related to recoil spectrum and damage energy should be comparable for 15-MeV and deuteron-breakup neutrons of the same mean energy.

ACKNOWLEDGMENTS

The authors wish to express their indebtedness to L. H. Jenkins who provided the experimental data for the range measurements. We also acknowledge helpful discussions with F. G. Perey and M. J. Saltmarsh.

References

- [1] L. H. Jenkins, G. J. Smith, J. F. Wendelken and M. J. Saltmarsh, this conference.
- [2] M. J. Saltmarsh and G. J. Smith, private communication.
- [3] M. T. Robinson, in: *Nuclear Fusion Reactors* (Brit. Nuclear Energy Soc., London, 1970), p. 364.
- [4] D. M. Parkin and A. N. Goland, Brookhaven (USA) Report, BNL 50434 (Sept. 1974).
- [5] ENDF/B is an Evaluated Nuclear Data File available from the National Neutron Cross Section Center, Brookhaven National Laboratory, Upton, New York 11973.
- [6] C. Y. Fu and F. G. Perey, to be published.
- [7] J. B. Roberto and M. T. Robinson, to be published.
- [8] J. Lindhard, V. Nielsen, M. Scharff and P. V. Thomsen, *Kgl. Danske Videnskab. Selskab, Mat-Fys. Medd.* 33, No. 10 (1963).
- [9] T. A. Gabriel, private communication.
- [10] L. H. Jenkins, T. S. Noggle, R. E. Reed, M. J. Saltmarsh and G. J. Smith, *Appl. Phys. Lett.* 26 (1975) 426.
- [11] R. Gähler, J. Kalus and R. Behrisch, *Nucl. Instr. Meth.* 130 (1975) 203.
- [12] K. B. Winterbon, *Ion Implantation Range and Energy Deposition Distributions*, Vol. 2 (IFI/Plenum, New York, 1975).
- [13] R. Behrisch, *Nucl. Instr. Meth.*, in press.
- [14] P. Sigmund, *Phys. Rev.* 184 (1969) 408.
- [15] J. B. Roberto, J. Narayan, and M. J. Saltmarsh, *Proc. of Int. Conf. on Radiation Effects and Tritium Technology for Fusion Reactors* (Gatlinburg, Tennessee, Oct. 1975), in press.

Table 1. Specific Damage Energies and Sputtering Yields for High Energy d-Be^a Neutrons in Cu, Nb and Au.

Material	Specific Damage Energy (x 10 ⁻²⁰ eV-cm ²)		Forward Sputtering Yields (x 10 ⁻⁵ atoms/neutron)	
	d-Be Neutrons	15 MeV Neutrons	Theory	Experiment ^b
Cu	27.6	30.1	3.3	---
Nb	25.2	26.6	1.4	<4.5
Au	19.8	21.2	2.2	2.8

^aDeuteron energy, 40 MeV

^bRef. 1

Table 2. Projected Ranges for (n,2n) Recoils in
Nb and Au Irradiated with d-Be^a Neutrons.

Material	Average Recoil Energy (keV)	Projected Range (Å)	
		Theory	Experiment
Nb	214	428	388
Au	92	96	112

^aDeuteron energy, 40 MeV.

Figure Captions

- Fig. 1 Neutron energy distributions for d-Be and d-Li sources for neutrons emitted in the forward direction. The distribution labelled EPR is for a typical first-wall in a d-T fusion reactor.
- Fig. 2 Primary recoil distributions resulting from (n,n') and (n,nx) reactions in Au for several neutron energies.
- Fig. 3 Specific damage energy vs. neutron energy for Cu, Nb and Au. For Au, the relative elastic and nonelastic contributions are shown.
- Fig. 4 Primary recoil distributions for d-Be and 15 MeV neutrons in Nb. A calculated recoil spectrum for a fusion reactor first-wall is also shown.
- Fig. 5 Primary recoil distributions for d-Be and 15 MeV neutrons in Cu and Au.
- Fig. 6 Schematic of the experimental arrangement for measuring ranges of radioactive recoils. In the figure, a representative range distribution function $F(x)$ is shown for a recoil starting at depth - x . The cross-hatched region represents the fraction of such recoils which would be emitted from the target.

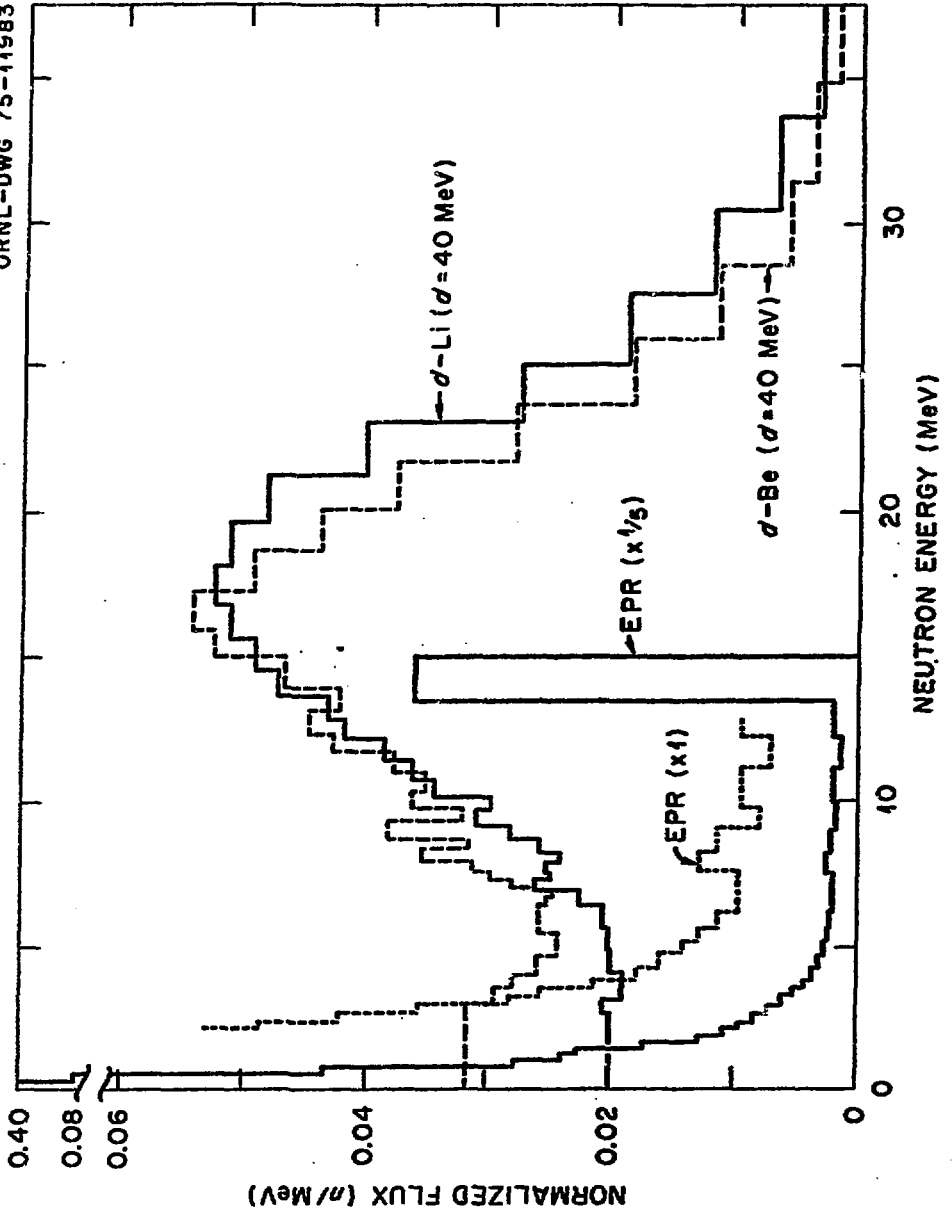
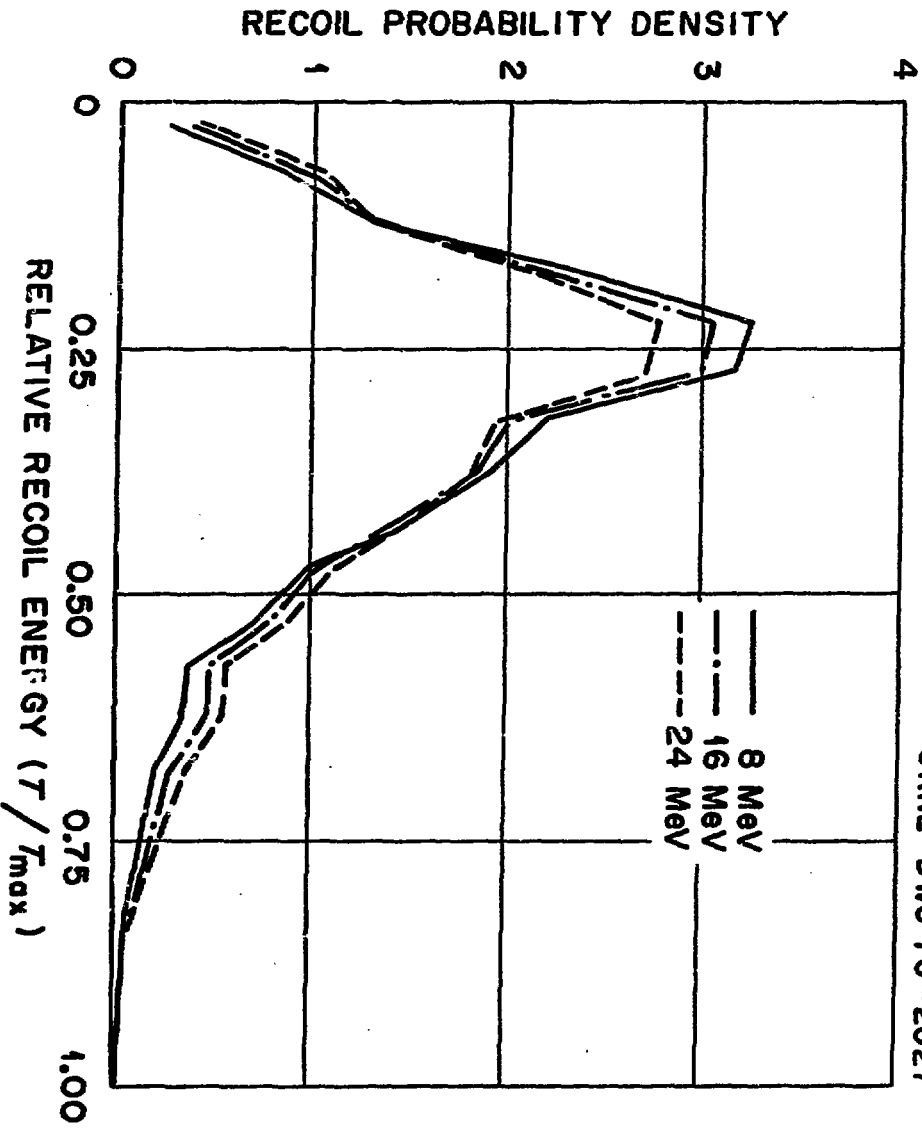


FIG. 1.



ORNL-DWG 76-2027

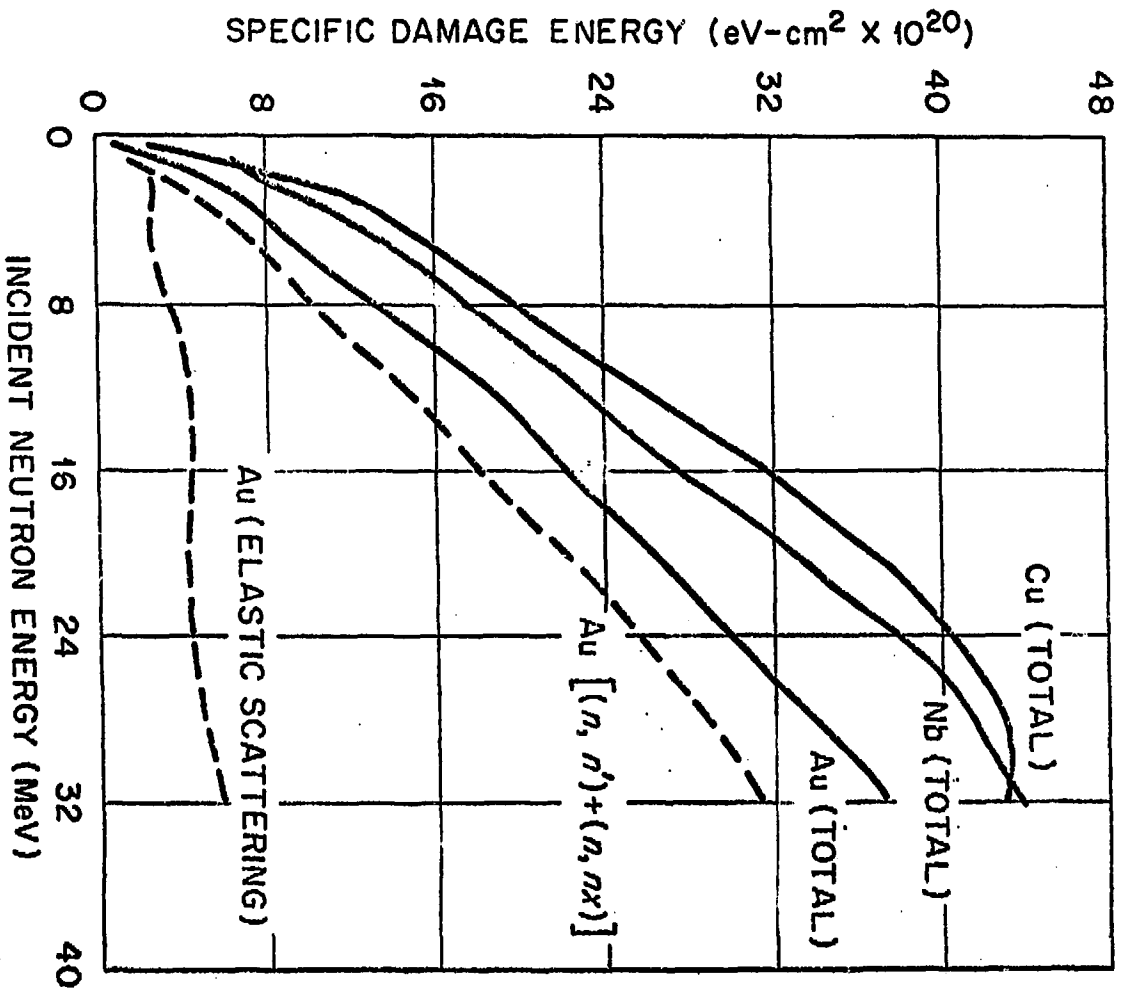
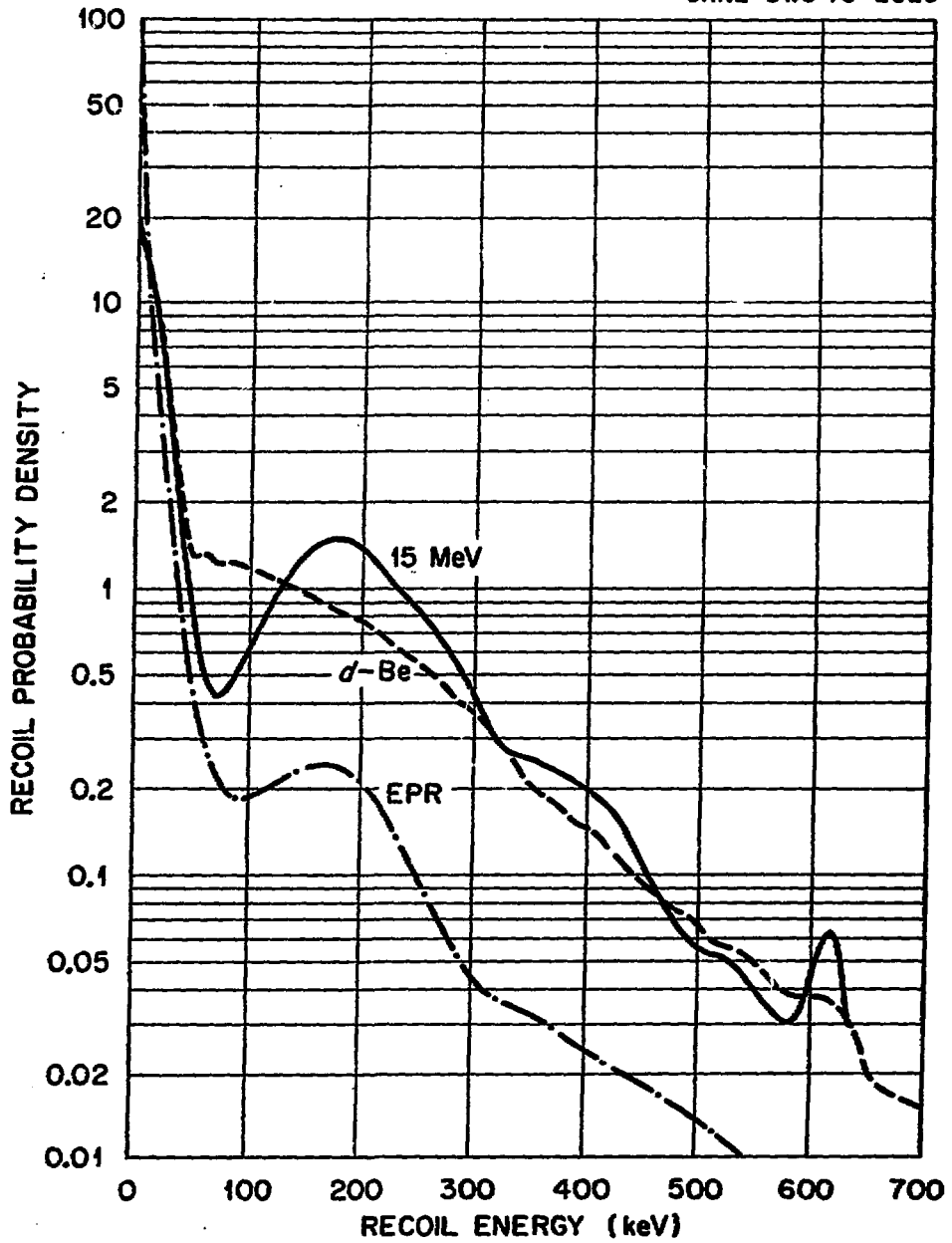
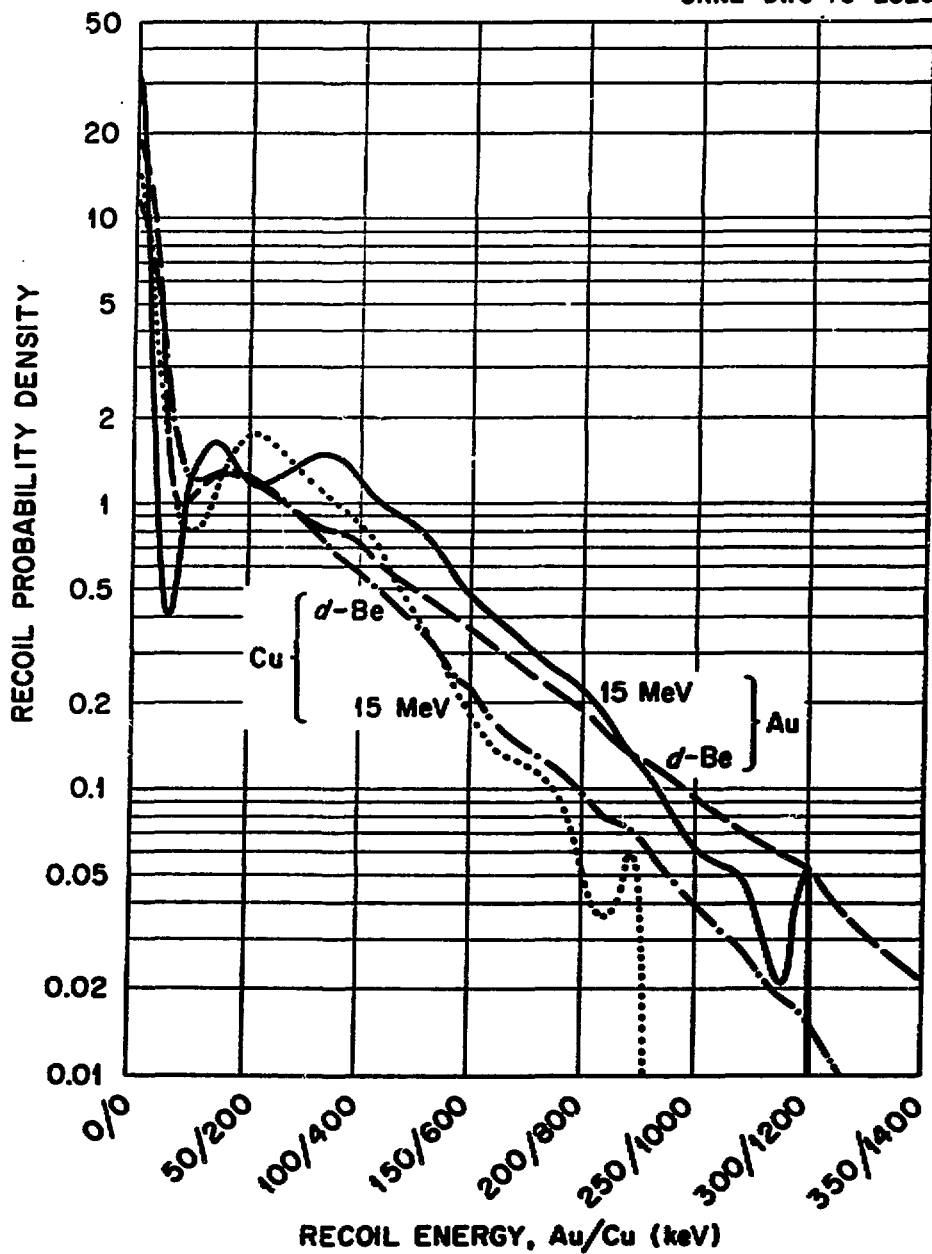


FIG. 3.





ORNL-DWG 76-2030

